

Collective sedimentation of colloids in grafted polymer layers

Tine Curk¹, Francisco J. Martinez-Veracoechea¹, Daan Frenkel¹, and Jure Dobnikar^{1,2}

¹*Department of Chemistry, University of Cambridge, Lensfield Road, CB2 1EW, Cambridge, UK*

²*Department for theoretical physics, Jožef Stefan Institute, Jamova 39, 1000 Ljubljana, Slovenia*

We present Monte Carlo simulations of colloidal particles pulled into grafted polymer layers by external fields. The insertion free energy of a single colloid into the polymer layer is qualitatively different for surfaces with an ordered and a disordered distribution of grafting points. Moreover, the tendency of colloidal particles to traverse the grafting layer is strongly size dependent. In dense colloidal suspensions, under the influence of sufficiently strong external force, a collective instability allows the colloids to penetrate and form internally ordered, columnar structures spanning the polymer layer. Depending on the conditions, these colloidal clusters may be isolated or laterally percolating. The morphology of the observed patterns can be controlled by the external fields, which opens up new routes for the design of thin structured films.

Grafted polymer layers can prevent the deposition of colloidal particles on solid surfaces, which is exploited in various applications like colloidal stabilisation, anti-fouling surfaces [1] and in biomedicine [2, 3]. Biological surfaces such as the lining of the intestine or the blood vessels walls are coated with polymers that inhibit the absorption of too large particles. Moreover, membrane-attached polymers over-expressed in cancer cells present a barrier for conventional drug delivery processes [4]. In several other applications, the insertion of colloids or nano-particles into polymer layers is exploited in order to fabricate functional responsive materials [5]: plasmonic nanostructures [6] convert chemo-physical forces into optical signals; ultrafast switches [7], organic memory devices [8] and advanced photovoltaics [9, 10] are based on incorporating metallic particles into polymers.

The physical properties of grafted polymer layers are governed by the configurational entropy of tethered polymers and have been studied extensively for different grafting and solvent conditions [11–14]. The penetration of particles into polymer layers has been recently addressed in theoretical and numerical studies [15, 16]. The insertion free energy of an isolated protein [17, 18] or colloid [19, 20] has been explored for varying grafting densities, particle sizes and shapes [21]. Colloids soluble in polymers penetrate up to a depth determined by their size [22], while insoluble particles form aggregates, which are expelled from the brush after reaching a critical size [23]. The polymer-mediated colloidal interactions are typically of the order of $k_B T$ [21, 24] (i.e., comparable to the entropic terms). The colloid-polymer mixtures are thus inherently less ordered than molecular systems. External forces could potentially be used to re-gain the order: due to the constrained translational degrees of freedom of the colloids pulled into the layers, the weak polymer-induced interactions could steer the assembly into ordered patterns. However, little is known about the collective particle sedimentation in a brush under the influence of a constant force.

Here we report Monte Carlo simulations of polymer-insoluble colloidal particles in grafted polymer layers. The system comprises of polymer chains end-grafted to a flat surface and hard sphere-colloids with diameter σ

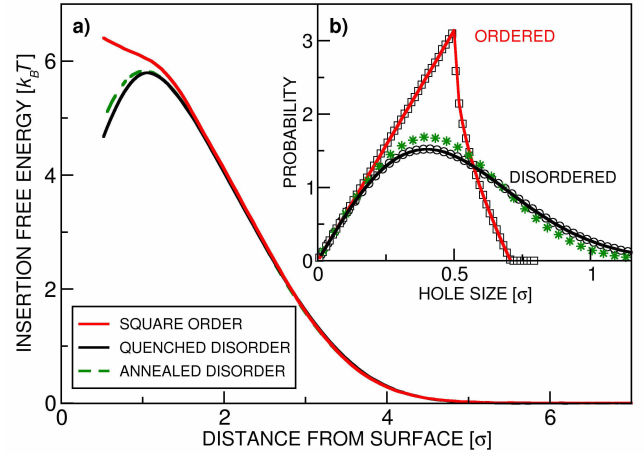


FIG. 1. Isolated colloids in polymer layers with grafting density $\rho = 1.0$ and number of blobs per chain $l_p = 20$. **(a)** The insertion free energy profile $F_p(z)$ for three realizations of the surface grafting: quenched disorder (black solid line), square crystalline order (red solid line), and annealed disorder (green dashed line). **(b)** The distribution of (2D) hole sizes for the three scenario. The solid lines represent the analytically derived expressions (see *Online SI*), symbols are numerically determined.

immersed in a neutral good solvent. The colloids interact via hard-core and polymer-mediated interactions and are additionally subject to a constant external force f_g , whose significance is measured by the ratio of potential versus thermal energy: $g' = f_g \sigma / k_B T$. A possible example of the external force is gravity: $f_g = g(\rho_c - \rho_s)\pi\sigma^3/6$, with $\rho_c - \rho_s$ the excess colloidal density in the solvent and g the standard gravitational acceleration. For gravity, the ratio $g' \propto \sigma^4$ strongly depends on the colloidal size: it is efficient for large-enough (micron-size) colloids and does not affect nano-particles or polymers in solution. Polymers can thus be treated as self-avoiding random walks. We follow a coarse-grained model [25] where the self-avoiding polymer chains are represented by l_p soft blobs with radius of gyration r_b [26]. The grafting density at the surface, $\tilde{\rho} = N_p/R_g^2$, determines whether

the layer is in the dilute “mushroom” ($\tilde{\rho} < 1$) or in the dense “brush” scaling regime ($\tilde{\rho} \gtrsim 3$) [27, 28]. We studied the transition regime with the mean spacing between the grafting points roughly similar to the polymer R_g [29]. Expressing the grafting density as number of anchors per colloidal diameter squared: $\rho = \tilde{\rho}R_g^2/\sigma^2$, we focused on the regime $0.5 < \rho < 5$, where the probability of inserting a colloid with $\sigma \approx R_g$ is non-vanishing.

The free energy profile $F(z)$ of a single colloid is the sum of its potential energy in the external field and the insertion free energy $F_p(z)$:

$$\beta F(z) = g' \frac{z}{\sigma} + \beta F_p(z). \quad (1)$$

The potential energy term is trivial and decouples from the polymeric degrees of freedom, therefore the insertion free energy is the key quantity governing the penetration of colloids into the polymer layers. We have used the above described coarse-grained model of polymers and evaluated the insertion free energy $F_p(z)$ by the Wang-Landau technique [30] for a wide range of polymer grafting densities ρ and number of blobs per chain l_p . In Figure 1(a) we compare polymer brushes characterized by ordered and disordered arrangement of the grafting points: $F_p(z)$ is plotted for layers with identical ρ but different spatial distribution of the grafting points: “quenched disorder” (random Poissonian process), “annealed disorder” (random grafting points relaxed before the simulation), and “order” (grafting points on a square lattice). The insertion free energy is qualitatively different in ordered and disordered case: the repulsion is strongest in case of ordered grafting where the free energy is monotonically decreasing with the height. In disordered case the free energy features a barrier. The height and position of the barrier and the depth of the minimum at the surface can be controlled (see *Online SI*), which enables reversible adsorption and slow release of the colloids at disordered surfaces.

The emergence of the free energy barrier (also observed in other simulations [15, 18]) is surprising: the mean monomer concentration profile is equal for ordered and disordered grafting and, at $\rho = 1.0$, it is monotonically decreasing with height (see *Online SI* and [16, 31]). The insertion free energy is obtained by exponential averaging of such profiles and is determined by both, the mean monomer concentration and its fluctuations. The fluctuations are characterized by the probability distribution of holes (regions void of monomers)[33]. In the inset (Figure 1(b)) the 2D hole-size distributions at the bottom surface are plotted: in case of disordered grafting characterized by the Poissonian statistics, there is an appreciable probability of finding large holes, while the ordered surfaces are characterized by small density fluctuations with a cut-off in the hole size. Close to the grafting surface the monomer fluctuations are “frozen” because the anchoring points are immobile, while away from it they relax: the surface-imposed effects vanish at a height equal to the characteristic length-scale [29].

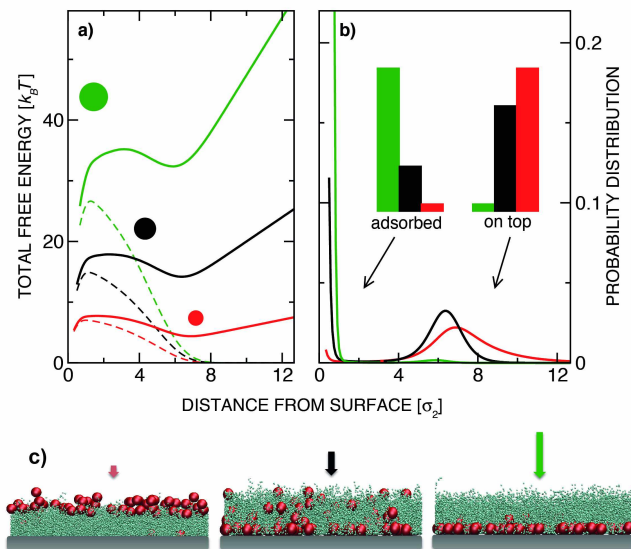


FIG. 2. (a) Total free energy (1) of sedimenting colloidal particles obtained by simulations at $l_p = 40$ and $\rho = 1.0$ for silica colloids with three sizes: $\sigma_1 = 0.67 \mu\text{m}$ (red line), $\sigma_2 = 1.00 \mu\text{m}$ (black line), and $\sigma_3 = 1.33 \mu\text{m}$ (green line). Respectively, $g'_2 = 2.0$ (corresponds to micrometer silica particles in water), $g'_1 = 0.40$ and $g'_3 = 6.3$. The dashed lines represent the insertion free energy $F_p(z)$. (b) Height distribution $P(z) \propto e^{-\beta F(z)}$ for the same system. The histograms illustrate the probability to find the colloids adsorbed to the surface or above the brush (left set of histograms: $z < R_g$ and right set: $z > R_g$). (c) Snapshots from Monte Carlo simulations of dilute colloidal suspensions at conditions corresponding to (a) and (b).

The free energy cost of inserting a particle into a disordered brush therefore initially grows as a function of height and eventually decreases along with the average monomer concentration - resulting in the barrier with a maximum around $z \approx R_g$. The barrier height scales with ρ and with σ^2 ; in our system its typical magnitude is several $10 k_B T$ (see *Online SI*).

The potential energy term (1) significantly alters the free energy landscape: for large enough g' the unstable local minimum becomes stable and the colloids are strongly confined to the surface. Since in the case of gravity g' sensitively depends on the colloidal size, this property can be used for particle-size sorting. In Figure 2 we plot the total free energy profiles (a) for colloids of three different sizes together with their height probability distribution (b). Counterintuitively, the smallest colloids gather on top of the brush (the gravity is too weak to overcome the steric barrier), while slightly larger colloids are distributed in a bimodal way and even larger ones are strongly confined to the bottom surface. This single-colloid picture also governs the density profiles in semi-dilute systems as seen in the simulation snapshots in Figure 2(c)). The amount of particles drawn into the polymer layer reflects the balance between the polymer-induced pressure pushing the

particles away and the external forces pulling them towards the surface. At a critical grafting density $\rho = \rho_0$ the two effects are balanced: for $\rho > \rho_0$ no particles can penetrate the polymer layer [34]. For $\rho < \rho_0$ the particles are pulled in the polymer layer by the excess external pressure - thereby displacing the polymers and increasing their effective density. When many colloids are inserted, the polymers mediate effective many-body interactions among the particles and the insertion free energy is no longer described by the single-particle term $F_p(z)$. In general it depends on the positions of all particles. To explore the multi-particle systems we have performed Grand-canonical Monte Carlo simulations with colloidal particles coupled to a reservoir with a fixed chemical potential at various polymer grafting densities, chain lengths, particle concentrations and external forces.

At large-enough pulling g' the penetrating particles start forming crystalline clusters at the bottom surface that grow towards the top of the brush [35]. Figure 3 shows typical growth scenarios on disordered and ordered surfaces. In the initial stages there is a difference: the shape of the clusters above the ordered surfaces is narrower at the bottom (resembling a table-top) due to the strong repulsion of colloids from the surface, while in case of disordered grafting the local free energy minimum enables pyramid-like structures. In both cases, however, similar final structures emerge: clusters with a uniform vertical profile spanning the brush from bottom to top resembling straight cylindrical towers. The maximum load of colloids in the polymer layer is achieved when the effective polymer density in the space around the colloids equals ρ_0 . Consequently, the thickness of a fully loaded layer $\propto \rho_0^{0.35}$ [11] does not depend on the polymer grafting density and can be controlled by inserting particles into the polymer layer (experimentally, an excessive amount of colloids could be added and the ones above the brush could be simply washed-off). Given the uniform vertical profiles observed in the colloidal clusters (Figure 3), the particle load is directly correlated to the colloidal surface coverage η of the two-dimensional horizontal cross-sections (top-view snapshots in Figure 4): $\eta \equiv S_{col}/S = 1 - \frac{\rho}{\rho_0}$, where S_{col}/S is the fraction of the area on the snapshot covered by the (red) colloids.

In Figure 4 we present the phase diagram as a function of the grafting density ρ and the critical density $\rho_0 \propto g'$. We have investigated both, ordered and disordered surfaces and observed no important differences in the lateral morphology. Different structures observed in the simulations are depicted by symbols and their phase boundaries are approximately marked by the solid lines, which are lines of constant colloidal surface coverage η . The white lower region of the diagram is the “super-critical” grafting region where no colloids penetrate the brush and no ordered structures are formed. The grey-shaded region depicts the regime where the colloids can penetrate the brush but the effective polymer density is too small and the entropy prevents particle ordering [36]. In order to understand the micro-phase separation leading to these

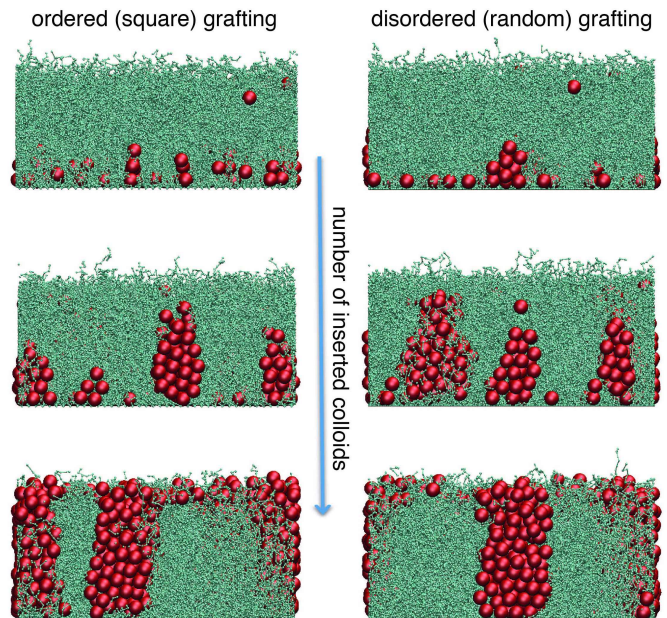


FIG. 3. Cluster growth as a function of the number of colloids in the system. Sedimentation sequence on ordered (left-hand side) and disordered (right-hand side) surfaces is depicted. Initially, “pyramid” and “table-top” structures are formed on disordered and ordered surfaces, respectively. Eventually, in both cases “critical” clusters with uniform vertical profiles spanning the polymer layer are formed. The number of blobs per chain is $l_p = 40$, the anchoring density $\rho = 4.0$, and the effective gravity $g' = 6.0$.

various patterns we consider two mechanisms: the depletion of polymers around solid objects that favours macro-phase separation, and an elastic-like penalty due to the fact that the polymers are grafted that promotes colloid-polymer mixing. The competition between such terms, combined with the action of the external forces, results in the formation of finite and ordered lateral patterns uniquely characterized by the colloidal surface coverage: at supercritical conditions ($\eta \equiv 0$) the colloids are in a liquid state on top of the brush; at small η isolated circular clusters emerge. Upon increasing the colloidal surface coverage snake-like objects, percolating structures and finally inverted clusters are formed. The morphologies are quite robust and are characterised by a well-defined length-scale (the width of the towers, snakes, or percolating structures). Interestingly, this length-scale does not depend on the grafting density but scales with l_p (i.e. with the polymer size) and is roughly equal to the brush height. The stability and properties of the reported patterns is reproduced by a phenomenological theory presented in *Online SI*.

Our results provide an insight into many-body polymer-induced particle interactions, which are of key relevance for understanding various biological processes, and to design novel materials and biomedical applications. Metal-coated micro-particles pulled into grafted

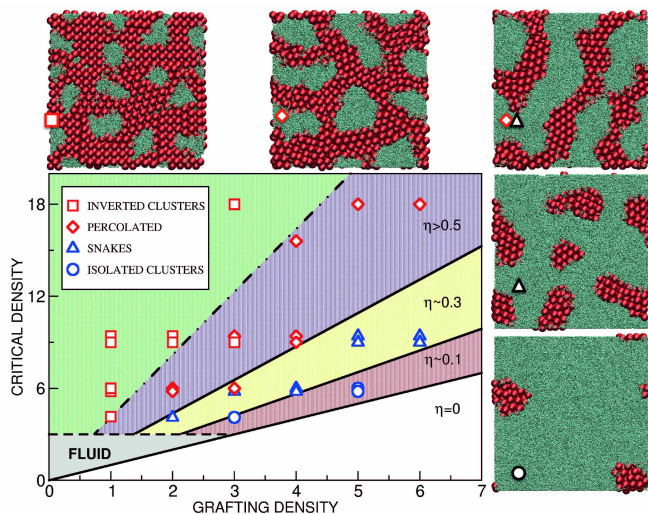


FIG. 4. Phase behaviour as a function of the polymer grafting density and the external pressure. Various lateral patterns are depicted by symbols: isolated cylindrical towers (blue circles), “snakes” (blue triangles), percolating structures (red diamonds) and inverted towers (red squares). The black lines of constant surface coverage η separating the phases are guides to the eye. Top-view snapshots from the simulations displaying the lateral morphology are shown at the side and marked by the same symbols. The snapshots are taken at an intermediate height within the polymer layer and correspond to the value of the critical density $\rho_0 = 6.0$ with $g' = 6.0$, $l_p = 40$ and the grafting density ranging from $\rho = 1.0$ (inverted towers) to $\rho = 5.0$ (isolated towers). The typical length-scale and the strong crystalline order are clearly revealed.

layers by gravity can form thin metallic films with unique mechanical, electric conductivity or heat transport properties. If mechanical stress can be applied to stretch or bend the substrate, the grafting density and the morphology of the emerging structures can be varied in a controlled way, which should provide a useful insight for surface characterization. We furthermore predict that grafted surfaces can be used as a sorting device for poly-disperse particles or particle aggregates, as well as to control the rates of chemical reactions. It has been shown [18] that the polymer brushes can affect protein folding processes, which is not surprising in light of our results. In order to fabricate the predicted multi-particle structures with nano- instead of micro-particles, ultra centrifuge can be used instead of gravity. The morphology of the reported structures is strongly desirable in modern nano-responsive applications like photovoltaics [37], smart glasses [7] and miniature sensors [38].

ACKNOWLEDGMENTS

We gratefully acknowledge enlightening discussions with Oren Scherman, Bortolo M. Moggetti, Patrick Varilly, Stefano Angioletti-Uberti, and Mark Miller. This work was supported by the 7th Framework Program of European Union through grants ARG-ERC-COLSTRUCTION 227758 (D.F., F.M.V., J.D.) and ITN-COMPLOIDS 234810 (J.D., T.C.), by the Erasmus student exchange program (T.C.), and by the Slovenian research agency through Grant P1-0055 (J.D.).

-
- [1] G. D. Bixler and B. Bhushan, *Biofouling: lessons from nature*, Philos. T. Roy. Soc. A 370 (2012) pp. 2381–2417
- [2] W. Senaratne, L. Andruzzi, and C. K. Ober, *Self-assembled monolayers and polymer brushes in biotechnology: Current applications and future perspectives*, Biomacromolecules 6 (2005), pp. 2427–2448
- [3] N. Ayres, *Polymer brushes: Applications in biomaterials and nanotechnology*, Polym. Chem. 1 (2010), pp. 769–777
- [4] X. Wang, A. A. Shah, R. B. Campbell, and K.-T. Wan, *Glycoprotein mucin molecular brush on cancer cell surface acting as mechanical barrier against drug delivery*, Appl. Phys. Lett. 97 (2010), pp. 263703-1–263703-3
- [5] M. A. Cohen Stuart, et al., *Emerging applications of stimuli-responsive polymer materials*, Nature Materials 9 (2010), pp. 101–113
- [6] I. Tokarev and S. Minko, *Tunable plasmonic nanostructures from noble metal nanoparticles and stimuli-responsive polymers*, Soft Matter 8 (2012), pp. 5980–5987
- [7] C. M. Lampert, *Large-area smart glass and integrated photovoltaics*, Sol. Energ. Mat. Sol. C. 76 (2003), pp. 489–499
- [8] By Y. Yang, J. Ouyang, L. Ma, R. Jia-Hung Tseng, and C.-W. Chu, *Electrical Switching and Bistability in Organic/ Polymeric Thin Films and Memory Devices*,
- [9] L. Gang, Z. Zhu, and Y. Yang, *Polymer solar cells*, Nature photonics 6 (2012), pp. 153–161
- [10] H. J. Snaith, G. L. Whiting, B. Sun, N. C. Greenham, W. T. S. Huck, and R. H. Friend, *Self-organization of nanocrystals in polymer brushes. Application in heterojunction photovoltaic diodes*, Nano Letters 5 (2005), pp. 1653–1657 Adv. Funct. Mater. 16 (2006), pp. 1001–1014
- [11] P.-G. de Gennes, *Scaling concepts in polymer physics*, Cornell University Press, 1979
- [12] S. T. Milner, T. A. Witten, and M. E. Cates, *Theory of the Grafted Polymer Brush*, Macromolecules, 21 (1988), pp. 2610–2619
- [13] B. Zhao, W. J. Brittain, *Polymer brushes: surface-immobilized macromolecules*, Prog. Polym. Sci. 25 (2000), pp. 677–710
- [14] J. R uhe, et al., *Polyelectrolyte Brushes*, Adv. Polym. Sci. 165 (2004), pp. 79–150
- [15] V. Ermilov and A. Lazutin, *Colloids in Brushes: The Insertion Free Energy via Monte Carlo Simulation with Umbrella Sampling*, Macromolecules 43 (2010), pp. 3511–3520
- [16] K. Binder, T. Kreerb, and A. Milchev, *Polymer brushes under flow and in other out-of-equilibrium conditions*, Soft Matter, 7 (2011), pp. 7159–7172

- [17] I. Szleifer, *Protein Adsorption on Surfaces with Grafted Polymers: A Theoretical Approach*, Biophys. J. 72 (1997), pp. 595–612
- [18] B. M. Rubenstein, I. Coluzza, and M. A. Miller, *Controlling the folding and substrate-binding of proteins using polymer brushes*, Phys. Rev. Lett. **108** (2012), pp. 208104
- [19] Y. Chen and J. Z. Y. Chen, *Absorption and engulfing transitions in nanoparticle infiltration into a polymer brush: A monte carlo simulation*, J. Polym. Sci. Part B Polym. Phys. 50 (2012), pp. 21–26
- [20] J. U. Kim and M. W. Matsen, *Repulsion Exerted on a Spherical Particle by a Polymer Brush*, Macromolecules 41 (2008) pp. 246–252
- [21] J. U. Kim and B. O’Shaughnessy, *Nanoinclusions in dry polymer brushes*, Macromolecules 39 (2006) pp. 413–425
- [22] J. U. Kim and B. O’Shaughnessy, *Morphology selection of nanoparticle dispersions by polymer media*, Phys. Rev. Lett. 89 (2002) pp. 238301-1–23801-4
- [23] O. A. Guskova, S. Pal, and C. Seidel, *Organization of nanoparticles at the polymer brush-solvent interface*, Europhys. Lett. 88 (2009), pp. 38006-p1–38006-p6
- [24] K. Chen and Y.-Q. Ma, *Interactions between Colloidal Particles Induced by Polymer Brushes Grafted onto the Substrate*, J. Phys. Chem. B 109 (2005), pp. 17617–17622
- [25] C. Pierleoni, B. Capone, and J.-P. Hansen, *A soft effective segment representation of semidilute polymer solutions*, J. Chem. Phys. 127 (2007), pp. 171102-1–171102-4
- [26] The blobs are connected with springs: $U_{ch}/k_B T = 0.534(r/r_b - 0.730)^2$ and repel via $U_{bb}/k_B T = 1.75 e^{-0.80(r/r_b)^2}$. They are also repelled from the colloids and surfaces via $U_{bc}/k_B T = 3.20 e^{-4.17(r/r_b - 0.50)}$.
- [27] K. Binder, *Scaling concepts for polymer brushes and their test with computer simulation*, Eur. Phys. J. E Soft Matter 9 (2002), pp. 293-298
- [28] E. Karaiskos, I. A. Bitsanis, and S. H. Anastasiadis, *Monte Carlo studies of tethered chains*, J. Polym. Sci. Part B Polym. Phys. 47 (2009), pp. 2449–2461
- [29] The relevant length scale in the dilute “mushroom” regime is the radius of gyration R_g of the chains. In the brush regime it is the so-called de Gennes blob (mean distance between the grafting points), $\xi \propto \rho^{-1/2}$ [11]. All our simulations are in the intermediate regime where the two length-scales are similar.
- [30] F. G. Wang and D. P. Landau, *Efficient, Multiple-Range Random Walk Algorithm to Calculate the Density of States*, Phys. Rev. Lett. 86 (2001), pp. 2050–2053
- [31] M. Murat and G. S. Grest, *Structure of a grafted polymer brush: a molecular dynamics simulation*, Macromolecules 22 (1989) pp. 4054–4059
- [32] I. Coluzza and J.-P. Hansen, *Transition from Highly to Fully Stretched Polymer Brushes in Good Solvent*, Phys. Rev. Lett. 100 (2008), pp. 016104-1–016104-4
- [33] M. A. Miller, R. Blaak, C. N. Lumb, and J.P. Hansen, *Dynamical arrest in low density dipolar colloidal gels*, J. Chem. Phys 130 (2009), pp. 114507-1–114507-12
- [34] The value of ρ_0 at a given externally applied force depends on the the solvent properties and on details of the colloidal and polymeric interactions. In our model the former are hard-core and the latter were chosen to describe the self-avoiding walk.
- [35] The colloidal insertion and deletion has been attempted with various rates. The attempted insertions were at random positions. However, most accepted insertions were on top of the brush and the colloids later diffused into the layer. At large ρ the system is frequently trapped in metastable states and the observed structures depend on the rate of the attempted insertions. At high rate, colloids form a layer on top compressing the polymers below them. If the effective density of polymers is thereby increased above critical ρ_0 , no colloids can penetrate. For slow-enough insertion, the colloids inserted on top have enough time to explore the free energy landscape and the system can reach the thermal equilibrium.
- [36] The extent of the fluid region depends on the physical parameters, especially on the colloidal excess density and size. Presented in Figure 4 is the case of $\sigma = 1\mu\text{m}$ silica colloids in water; for smaller colloids the boundary of the fluid region would shift upwards.
- [37] R. Oren, Z. Liang, J. S. Barnard, S. C. Warren, U. Wiesner, and W. T. S. Huck, *Organization of nanoparticles in polymer brushes*, J. Am. Chem. Soc. 131 (2009) pp. 1670–1671
- [38] J. Zhang, R. J. Coulston, S. T. Jones, J. Geng, O. A. Scherman, and C. Abell, *One-Step Fabrication of Supramolecular Microcapsules from Microfluidic Droplets*, Science 335 (2012), pp. 690–694